ELSEVIER

Catalysis Today 33 (1997) 49–56

CATALYSIS TODAY

New precursors to vanadium phosphorus oxide catalysts

Jay B. Benziger *, Vadium Guliants [1], Sankaran Sundaresan

Department of Chemical Engineering, Princeton University, Princeton, NJ 08544-5263, USA

Abstract

New precursors to vanadium phosphorus oxide catalysts have been synthesized based on alteration of the layered structure found in the active VPO catalysts. n-Alkyl amine intercalation compounds of vanadyl hydrogen phosphate hemihydrate have been prepared that are transformed into active vanadyl pyrophosphate catalysts. Catalytic performance for selective oxidation of n-butane to maleic anhydride improves with length of alkyl chain. Vanadyl phosphonates and vanadyl phosphite have been prepared containing vanadyl dimer structures that are thermally transformed into vanadyl pyrophosphate below 650 K for the phosphonates and 550 K for the phosphite. The VPO catalyst from the vanadyl phosphite precursor had a high surface area of 35 m^2/g, and displayed better selectivity for maleic anhydride from n-butane oxidation than the conventional unpromoted catalyst. Mixed vanadyl phosphite–phosphate materials, which were found to be very reactive for intercalation of amines, were intercalated with 3-aminopropyltriethoxysilane and calcined to produce the first thermally stable pillared VPO catalyst.

1. Introduction

Vanadium serves as an important oxidation catalyst in both chemical and biochemical systems [1–4]. The utility of vanadium as a catalysts stem from its facile inter-conversion among the higher oxidation states of vanadium and its ability to activate molecular oxygen [5].

The 14-electron selective oxidation of n-butane to maleic anhydride (2,5-furandione) on vanadium–phosphorus–oxide (VPO) catalysts is the only industrial significant process of selective oxidation of an alkane [6–8], and one of the most fascinating and unique heterogeneous catalytic processes. Bergman and Frisch first reported the selective oxidation of n-butane to maleic anhydride by VPO in 1966 [9], and since commercialization in 1974 this route has replaced the use of benzene in over 70% of maleic production worldwide [10]. Under typical conditions a 2 mol% n-butane in air feed is converted to maleic anhydride over an unsupported VPO catalyst at 673–723 K and space velocities of 1100–2600 h^{-1}. Typical selectivities for maleic anhydride of commercial catalysts are 65–75% at 70–85% n-butane conversions.

VPO catalysts for n-butane oxidation have been extensively characterized, and the most selective catalysts consist principally of crystalline vanadyl(IV) pyrophosphate (VPP), $(VO)_2P_2O_7$ [11,12].

The vanadyl pyrophosphate is derived from vanadyl hydrogen phosphate hemihydrate (VHP), $VOHPO_4 \cdot 0.5H_2O$, by calcination and

* Corresponding author. Tel.: +1-609-2585416; fax: +1-609-2580211; e-mail: benziger@princeton.edu.

[1] Present address, Praxair, Tonawanda, NY.

PII S0920-5861(96)00135-6

subsequent aging under reaction conditions. Various routes are available to prepare the VHP precursor, as outlined in Fig. 1. The aqueous route entails the reduction of V^{5+} by $NH_2OH \cdot HCl$ or other reducing agents followed by the addition of phosphoric acid. $VOHPO_4 \cdot 0.5H_2O$ is recovered by crystallization or evaporation. The organic route involves the reduction of V_2O_5 by an organic solvent (an alcohol), followed by the reaction with phosphoric acid and recovery of the solid. After recovery of the VHP precursor, it is washed to remove trace amounts of water soluble V^V compound and then calcined in nitrogen at 773 K, followed by final activation in air or n-butane/air at 673 K. It is critical that calcination and activation be carefully controlled or the catalyst can be over oxidized resulting in the formation of $VOPO_4$, which is a non-selective catalyst for n-butane.

The synthesis route, and the reaction conditions during synthesis affect the morphology of the $VOHPO_4 \cdot 0.5H_2O$, and ultimately the catalyst performance. The VHP precursor prepared by the aqueous synthesis route are generally more crystalline (as defined by X-ray diffraction) than the catalysts prepared by the organic route [7,8,13]. The organic synthesis route results in platelet crystalline morphology; the size of the platelets and the way they pack are determined by the choice of organic solvent. Isobutanol produces a rosette morphology where the platelets agglomerate. With sec-butyl or t-butyl alcohol well formed platelets form that do not agglomerate [12]. The crystal ordering of the hemihydrate is also affected by the solvent. Large alcohols, such as benzyl alcohol, appear to produce platelets with stacking faults, deduced from the broadening of the (200) reflection in the XRD [12,13]. Stacking fault defects in the $VOHPO_4 \cdot 0.5H_2O$ precursor have been

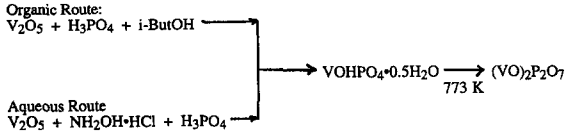

Fig. 1. Synthesis routes for vanadyl pyrophosphate catalysts.

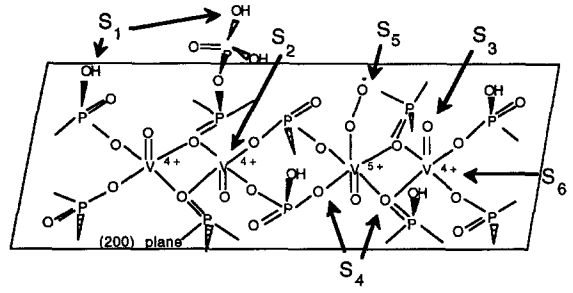

Fig. 2. Termination of the (200) plane of vanadyl pyrophosphate and proposed active sites for oxidation. Active sites proposed to exist on the vanadyl pyrophosphate surface. (S_1) Brønsted acid site; (S_2) Lewis acid site; (S_3) terminal oxygen; (S_4) bridging oxygen; (S_5) η^2-superoxo or η^1-peroxo site; (S_6) V^V/V^{IV} redox couple.

correlated with improved catalyst performance [14].

The active sites for n-butane oxidation has been proposed as being the (200) plane of vanadyl pyrophosphate. Crystallites that preferentially expose the (200) plane have been found to exhibit higher selectivities for n-butane oxidation [7]. Transmission electron microscopy has shown that catalyst selectivity correlated with the disappearance of an amorphous surface layer on vanadyl pyrophosphate platelets [15]. Seven different types of active sites have been suggested for the (200) plane of vanadyl pyrophosphate catalysts, shown in Fig. 2: (i) Brønsted acid sites, probably –POH groups, (ii) Lewis acid sites, probably V^{IV} and V^V, (iii) one electron redox couples, V^V/V^{IV}, V^{IV}/V^{III}, (iv) two electron redox couple V^V/V^{III}, (v) bridging oxygen, V–O–V, or V–O–P, (vi) terminal oxygen $V^V{=}O$, $V^{IV}{=}O$ and (vii) activated molecular oxygen η^1-peroxo and η^2-superoxo species. Centi et al. [7] have suggested that the vacant apical coordination site on the vanadium in the vanadyl dimer V_2O_8 is a Lewis acid site for a methylene hydrogen atom abstraction. Grasselli et al. [16] have suggested that this vacant coordination site on the vanadyl dimers activates molecular oxygen forming surface-bound η^1-peroxo and η^2-superoxo species; a 'pseudo-ozonide' species formed by the interaction of a chemisorbed O_2 molecule and an

adjacent V = O moiety is suggested as activating n-butane.

The critical feature of the (200) surface of vanadyl pyrophosphate for selective oxidation of n-butane appears to be the vanadyl dimer. Other vanadium phosphates, such as $VOPO_4$ are capable of selectively oxidizing olefins, such as 1-butene or butadiene to maleic anhydride, but these other VPO phases lead to almost total combustion of n-butane [17]. The vanadyl dimer at the surface has a ligand missing from one of the vanadium center in the dimer structure, and the belief is that vanadium can activate the C–H bond in n-butane [7,18,16].

Vanadyl hydrogen phosphate hemihydrate, the precursor to the active pyrophosphate catalysts also is composed of vanadyl dimers, and it has been suggested by Bordes that the hemihydrate precursor is converted to the pyrophosphate phase by a topotactic process [19]. Ebner and Thompson have questioned the idea of a topotactic conversion because the orientation of the two apical oxygen change during the conversion, and amorphous phases are observed at intermediate stages during the conversion [20]. Nevertheless, the vanadyl dimers are still identified as crucial for the activation of alkanes.

In the existing patent and scientific literature there is a vast array of procedures outlined for synthesizing vanadyl hydrogen phosphate hemihydrate and the subsequent conversion into an active vanadyl pyrophosphate catalyst [6,21,7,8]. These procedures involve aqueous and organic media for the synthesis, different reducing agents, additives that facilitate crystal growth and granularity, promoters for the catalyst, etc. Except for some recent work by Moser using an aerosol technique to directly prepare VPO catalysts [22], all the preparation techniques have been based on the vanadyl hydrogen phosphate hemihydrate precursor. We have recently developed new types of precursors for VPO catalysts based on intercalation compounds, and V^{IV}–P^{III} compounds, that have produced active and selective partial oxidation catalysts. In several cases we have synthesized new materials that have exhibited superior performance to catalysts prepared by existing patent procedures. The conceptual construct for these new materials and the procedures for preparation are presented here.

2. Intercalated vanadyl hydrogen phosphate hemihydrate as VPO catalyst precursors

VPO oxidation catalysts are generally unsupported (the one exception is the new DuPont fluidized bed process which will use a modified type of supported catalyst to improve attrition resistance [23]). The surface areas are quite modest, typically in the range of 10 m^2/g. A fact that had not been widely appreciated, nor exploited is that the vanadyl hydrogen phosphate hemihydrate precursor is a layered compound. By forcing the layers apart and inserting pillars, the active surface area of the catalyst could be increased.

Vanadyl hydrogen phosphate hemihydrate ($VHP–VOHPO_4 \cdot 0.5H_2O$) was prepared by the standard patent procedure in an alcohol medium [18,16]. After washing the VHP in acetone and drying at 423 K for 2 h, C_3–C_6 n-alkyl amines were intercalated by heating 1 g of VHP in a large excess of the neat amine for 7–10 days. Longer chain amines and secondary or tertiary amines did not intercalated directly into the VHP lattice. However, C_7–C_{12} primary amines could be exchanged into VHP intercalated with n-amyl or n-hexyl amine by refluxing the intercalated VHP in a large excess of the neat amine. Ammonia was also intercalated into VHP by passing gaseous ammonia over the VHP at room temperature for 24 h.

The inter-layer spacing in the (100) direction increased linearly with the length of the alkyl chain as the alkyl amines formed a close-packed interlayer structure with the amino groups bonding to POH groups and structural water molecules (see Table 1). The stoichiometry of intercalation yielded 1.5 amines per VHP unit indicating hydrogen bonding of the amines with

Table 1
Properties of vanadyl hydrogen phosphate hemihydrate intercalated with n-alkylamines ($VOHPO_4 \cdot 0.5H_2O \cdot xRNH_2$)

Base	d_{001} (Å)	x (CHN analysis)	Catalytic selectivity for maleic anhydride [a]
Ammonia	7.38	1.71	19% (28%)
Propylamine	14.70	1.63	22% (36%)
n-Butylamine	16.11	1.64	27% (32%)
n-Hexylamine	20.38	1.57	44% (34%)
n-Octylamine	25.09	1.73	50% (31%)

[a] Numbers in parentheses are n-butane conversion. Reaction conditions are 675 K and GHSV 700 h^{-1}.

both POH groups and structural water groups as shown in Fig. 3. Unfortunately, the interlayer bonding was too strong to permit substitution of the alkyl amines with silicon amines that would be the basis of thermostable pillars. The n-alkyl amine intercalated hemihydrate species were thermally converted to vanadyl pyrophosphate catalysts, and tested for the oxidation of n-butane. The intercalated VHP precursors were activated in a 1.2% n-butane in air mixture at 698 K for 4 days after which the temperature was decreased to 673 K and the conversion of n-butane to maleic anhydride, carbon oxides and C_2 acids was measured. The results, which are summarized in Table 1, show these are selective partial oxidation catalysts though they perform poorer than a commercial catalyst. The results also show an increase in catalyst selectivity with increasing chain length of the intercalated amine. This increase in selectivity is suggested to arise from stacking disorders created in the vanadyl pyrophosphate due to the larger interlayer spacing in the catalyst precursor.

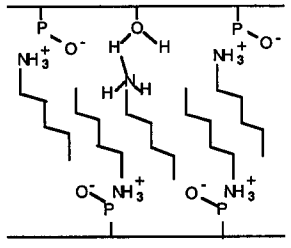

Fig. 3. Proposed arrangement of n-amylamine bilayers in $VOHPO_4 \cdot 0.5H_2O$ along the (100) direction. An acid–base adduct is formed with POH groups, while structural water is proposed to hydrogen bond to the amine.

3. Vanadyl phosphonates as VPO catalyst precursors

To permit intercalation of thermally stable pillar materials, it appeared to be necessary to weaken the interlayer bonding in the precursor, suggesting the desirability of replacing the hydroxyl groups of the POH groups with more weakly interacting groups such as alkyl groups, as shown in Fig. 4.

Johnson and co-workers reported the synthesis of vanadyl methyl, ethyl and propyl phosphonates $VOC_nH_{2n+1}PO_3 \cdot H_2O$ ($n = 1$–3), V^{IV}–P^{III} compounds with POH groups replaced by PR groups [24]. This synthesis was analogous to the synthesis of VHP, but introduced the phosphorus via a phosphonic acid ester, rather than phosphoric acid. Based on magnetic susceptibility data Johnson concluded that the methyl and ethyl phosphonates contained vanadyl dimers analogous to the structure in vanadyl hydrogen phosphate hemihydrate. Johnson suggested that for alkyl groups smaller than the OH group the preferred structure contains vanadyl dimers, whereas for larger groups single vanadyl octahedra are preferred.

Following the lead of Johnson we synthesized series of vanadyl phosphonates from $n =$ 0–4 and phenyl phosphonate. Vanadium pentoxide was refluxed in anhydrous ethanol for 16 h to reduce the vanadium to V^{IV}. Phosphorus acid or phosphonic esters dissolved in anhydrous ethanol was added to achieve a P/V ratio

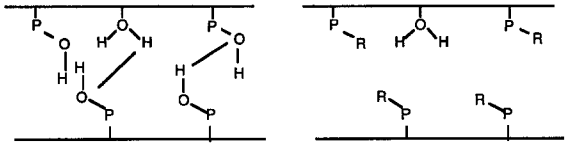

Fig. 4. Schematic showing the hydrogen bonding interactions between layers of vanadyl hydrogen phosphate hemihydrate and the proposed concept to replace the OH groups with alkyl groups to reduce the interlayer bonding.

of 1.0–1.3. The reaction mixture was refluxed for another 20 h. Light blue solids were recovered by filtration and were washed with ethanol and acetone and dried in air. Elemental analyses were consistent with the formula $VOC_nH_{2n+1}PO_3 \cdot xH_2O$ ($n = 0$–4, $x = 1$ or 1.5).

Powder X-ray diffraction patterns indicated these were layered compounds with the layer spacing increasing with increasing carbon chain length (see Table 2).

Magnetic susceptibility measurements were collected between 4 and 300 K on a SQUID magnetometer (see Fig. 5). The magnetic susceptibility of all the linear alkyl phosphonate samples and showed a maximum circa 50 K indicative of spin exchange in vanadyl dimers. No maximum in magnetic susceptibility was observed with the phenyl phosphonate indicating its structure contained only isolated vanadyl octahedra.

Vanadyl phosphite ($VOHPO_3 \cdot 1.5H_2O$) and the alkyl phosphonates were all found to have the same vanadyl dimer structure of vanadyl hydrogen phosphate hemihydrate, and the interlayer spacing increased linearly with the length of the alkyl chain [25]. Vanadyl phosphite and the vanadyl alkyl phosphonates were all transformed to vanadyl pyrophosphate upon calcination in air, with the degree of crystalline ordering decreasing with increasing alkyl chain length. The most significant result was the ease of this transformation. Vanadyl ethyl, propyl and butyl phosphonate were converted to vanadyl pyrophosphate below 650 K, over 100 K lower than the temperature required to transform vanadyl hydrogen phosphate hemihydrate, and vanadyl phosphite was converted to vanadyl pyrophosphate below 550 K! This dramatic re-

Table 2
Interlayer spacing and elemental compositions for vanadyl phosphonates ($VOC_nH_{2n+1}PO_3 \cdot xH_2O$)

n	0	1	2	3	4
d_{001} (Å)	7.28	8.32	9.73	11.19	12.29
V (%)	28.26	27.56	23.78	23.16	21.77
P (%)	15.93	17.30	15.33	14.52	12.65
C (%)	0.77	6.98	12.51	16.69	21.83
x	1.75	1.65	1.53	1.51	1.06

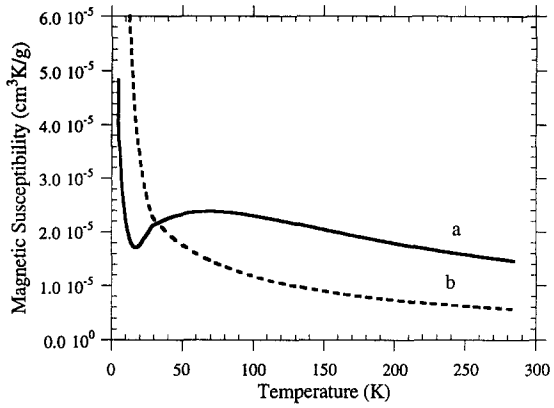

Fig. 5. Magnetic susceptibility data for (a) vanadyl(IV) phosphite ($VOHPO_3 \cdot 1.5H_2O$); (b) vanadyl(IV) phenyl phosphonate ($VO(C_6H_5)PO_3 \cdot H_2O$). The data have been fit to Bleaney–Bowers expressions $\chi = \chi_0 + C_i/(T - \Theta) + 4C_d/(T(3 + \exp(-2J/k_BT)))$, with parameters {vanadyl phosphite ($C_d(1.9\times10^{-3}$ cm^3 K/g), $2J/k_B$ (−84.5 K), C_i (23.6×10^{-5} cm^3 K/g), Θ (−1.0 K), χ_0 (9.87×10^{-7} cm^3 K/g), μ_{eff} (1.73 μ_B)}, {vanadyl phenyl phosphonate ($C_d(0.1\times10^{-3}$ cm^3 K/g), $2J/k_B$ (−68.5 K), C_i (5.2×10^{-5} cm^3 K/g), Θ (4.0 K), χ_0 (-8.8×10^{-7} cm^3 K/g), μ_{eff} (1.75 μ_B)}.

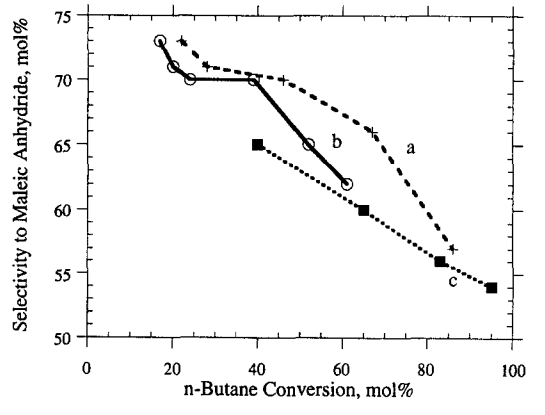

Fig. 6. Conversion and selectivity for n-butane oxidation over VPO catalysts derived from vanadyl phosphite (a) and vanadyl methylphosphonate (c) precursors compared with conventionally prepared VPO catalyst derived from vanadyl hydrogen phosphate hemihydrate (b). Reaction carried out at 654 K in 1.2% n-butane in air.

duction in the temperature required for conversion can significantly reduces the possibility of over-oxidation of the VPO catalyst to V^{5+} phases ($VOPO_4$) and could have significant impact on the catalytic activity of the VPO catalysts.

The catalytic performance of vanadyl pyrophosphate derived from vanadyl phosphite synthesized at different P/V ratios and vanadyl methylphosphonate were examined for n-butane oxidation to maleic anhydride and compared to a conventionally prepared VPO catalyst derived from vanadyl hydrogen phosphate hemihydrate. The results shown in Fig. 6 indicate that the VPO catalyst from the vanadyl phosphite precursor had higher selectivity to maleic anhydride at higher conversions than the conventional catalyst. Furthermore, the surface area of the catalyst derived from vanadyl phosphite was 44 m^2/g, more than twice that for the conventional catalyst.

4. Intercalated mixed vanadyl phosphite–vanadyl hydrogen phosphate hemihydrate as VPO catalyst precursors

Further modifications of the vanadyl phosphite were attempted by intercalation of amines. n-Alkyl amines intercalated into vanadyl phosphite forming single or double layer structures depending on the amine concentration in solution. However, the interlayer bonding was found to be too great to permit intercalation of bulky aminoalkoxy-silanes to serve as pillars. The interlayer bonding was further weakened by preparing randomly mixed vanadyl phosphate–phosphite materials, $VO(HPO_4)_y(HPO_3)_{1-y} \cdot 2H_2O$.

V_2O_5 was refluxed in anhydrous ethanol for 16 h. At that time a mixture of orthophosphoric and phosphorus acids were added to give a synthesis P/V ratio of 1, and $y = 0.5$ or 0.75. The reaction mixture was refluxed for another 20 h. Light blue solids were isolated by filtration, washed with ethanol and acetone and dried in air. Elemental analyses for the two samples were: $y = 0.75$, V: 26.70% (27.38%), P: 16.74% (16.64%), $x(H_2O)$, $x = 2.02$; $y = 0.50$, V: 26.20% (26.70%), P: 16.40% (16.23%), $x(H_2O)$, $x = 2.08$.

Intercalated phases were prepared by contacting the host with a two-fold excess of 0.2 M t-butylamine or 0.5 M 3-aminopropyltriethoxysilane (APS) in anhydrous ethanol at room temperature for 48 h. Pillared material was obtained by calcining the APS-intercalated phase in nitrogen at 673 K for 2 h.

The XRD patterns of the mixed phases corresponded to layered solids with low crystalline order. Only two reflections were observed: the (001) peak corresponding to the interlayer spacings of 8.14 Å ($y = 0.75$) and 9.58 Å ($y = 0.50$), and the (220) peak associated with the most intense in-layer reflection at ca. 2.9 Å. The absence of other hk0 reflections indicated no long range order in the *ab* plane suggesting random distribution of the phosphite and phosphate groups.

The mixed phosphate–phosphite exhibited increased interlayer spacing (8.14 Å) relative to both vanadyl hydrogen phosphate hemihydrate (5.69 Å) and vanadyl phosphite (7.27 Å) as a result of weaker interlayer bonding. The weaker interlayer bonding permitted intercalation of *t*-butyl amine, which could not be intercalated into either of the pure components. 3-Aminopropyltriethoxysilane (APS) was intercalated into a mixed layer compound, $VO(HPO_4)_{0.25}(HPO_3)_{0.75} \cdot 2H_20$ increasing the layer spacing from 8.14 to 20.16 Å. After calcination of the APS intercalated compound in nitrogen at 673 K the layers remained separated by 17.0 Å, representing the first thermally stable pillared VPO. Above 723 K, the APS intercalated compound converted into a vanadylpyrophosphate with several V^V impurity phases present.

The catalytic performance of the pillared VPO was tested for n-butane oxidation at 673 K. The initial selectivity for maleic anhydride was very

low, < 10%, and a steady selectivity of 25% was achieved after 6 days on stream with a conversion of 45%.

5. Conclusions

New approaches to VPO catalyst precursors for n-butane oxidation have been described based on altering their layered structure. The conventional precursor, vanadyl hydrogen phosphate hemihydrate was intercalated with n-alkyl amines which altered the stacking order in the vanadyl pyrophosphate catalysts derived from these precursors. By increasing the distance between layers in the precursor the selectivity of the catalyst was improved. Vanadyl phosphonates containing vanadyl dimers were synthesized to reduced the interlayer bonding in the precursors. These materials could be converted into vanadyl pyrophosphate catalysts at substantially lower temperatures than the conventional hemihydrate precursor, and gave catalysts with higher surface areas and improved yields of maleic anhydride. Mixed vanadyl phosphite–vanadyl hydrogen phosphate materials were synthesized that served as a host to aminopropyltriethoxysilane which produced a thermally stable pillared VPO catalyst.

Acknowledgements

This work was supported by the National Science Foundation and the Amoco Chemical Company. We wish to specially thank John Forgac and Muin Haddad of Amoco Chemicals for their helpful suggestions and support thorough this work.

References

[1] Vanadium in Biological Systems (Kluwer, Dordrecht, 1990) p. 63.
[2] B.J. Hales, E.E. Case, J.E. Morningstar, M.F. Dzeda and L.A. Mauterer, Biochemistry 25 (1986) 7251.
[3] S.G. Brand, C.J. Hawkins and D.L. Parry, Inorg. Chem. 26 (1987) 629.
[4] B. Borah, C.-W. Chen, W. Egan, M. Miller, A. Wlodawer and J.S. Cohen, Biochemistry 24 (1985) 2058.
[5] R.A. Sheldon and J.K. Kochi, Metal Catalyzed Oxidations of Organic Compounds (Academic Press, New York, 1981).
[6] F. Cavani and F. Trifirò, Appl. Catal. 88 (1992) 115; G. Centi, ed., Catal. Today 16 (1993); J.R. Ebner and M.R. Thompson, In: eds. R.K. Grasselli and A.W. Sleight, Structure-Activity and Selectivity Relationships in Heterogeneous Catalysis (Elsevier, Amsterdam, 1991) p. 31; R.M. Contractor, J.R. Ebner and M.J. Mummy, In: eds. G. Centi and F. Trifirò, New Developments in Selective Oxidation (Elsevier, Amsterdam, 1990) p. 553.
[7] G. Centi, F. Trifirò, J.R.I. Ebner and V.M. Franchetti, Chem. Rev. 88 (1988) 55.
[8] F. Cavani and F. Trifirò, Catalysis 11 (1994) 246.
[9] R.I. Bergman and N.W. Frisch, US Patent 3,293,268, 1966.
[10] J.I. Kroschwitz and M. Howe-Grant, In: Encyclopedia of Chemical Technology (Wiley, New York, 1991).
[11] I. Matsuura, Catal. Today 16 (1993) 123; T. Okuhara and M. Misono, Catal. Today 16 (1993) 61; L.M. Cornaglia, C.A. Sanchez and E.A. Lombardo, Appl. Catal. 95 (1993) 117; E. Bordes, Catal. Today 16 (1993) 27; D. Ye, A. Satsuma, A. Hattori, T. Hattori and Y. Murakami, Catal. Today 16 (1993) 27.
[12] H.S. Horowitz, C.M. Blackstone, A.W. Sleight and G. Teufer, Appl. Catal. 38 (1988) 193.
[13] S. Urvin-Monshaw and A. Klein, Chem. Eng. 96 (1989) 35.
[14] L.M. Cornaglia, C.A. Sanchez and E.A. Lombardo, Appl. Catal. A: General 95 (1993) 117.
[15] V.V. Guliants, J.B. Benziger, S. Sundaresan, N. Yao and I.E. Wachs, Catal. Lett. 32 (1995) 379.
[16] P.A. Agaskar, L. DeCaul and R.K. Grasselli, Catal. Lett. 23 (1994) 339.
[17] E. Bordes, In: eds. R.K. Grasselli and A.W. Sleight, Structure-Activity and Selectivity Relationships in Heterogeneous Catalysis (Elsevier, Amsterdam, 1991) p. 21; I. Matsuura and M. Yamazaki, In: eds. G. Centi and F. Trifirò, New Developments in Selective Oxidation (Elsevier, Amsterdam, 1990) p. 563; F.B. Abdelouahab, R. Olier, N. Guilhaume, F. Lefebvre and J.C. Volta, J. Catal. 134 (1992) 151.
[18] B. Schiøtt, K.A. Jørgensen, R. Hoffman, J. Phys. Chem. 95 (1991) 2297.
[19] E. Bordes, Catal. Today 1 (1987) 499; E. Bordes, J.W. Johnson and P. Courtine, J. Solid State Chem. 55 (1984) 270.
[20] M.R. Thompson, A.C. Hess, J.C. White, J. Anchell, J.B. Nicholas, M.I. McCarthy, J.R. Ebner and F.W. Lytle, II World Congr. and IV Eur. Workshop Meet. on New Developmens in Selective Oxidation, Benalmadena, Spain, 1993.
[21] R.M. Contractor, H.E. Bergna, H.S. Horowitz, C.M. Blackstone, B. Malone, C.C. Torardi, B. Griffiths, U. Chowdhry and A.W. Sleight, Catal. Today 1 (1987) 49; J.P. Harrison, US Patent 4064070, 1977.
[22] W.R. Moser, In: eds. J. Hightower and T. Oyama, Catalytic Selective Oxidation (Am. Chem. Soc., 1993) p. 244.

[23] J. Haggin, Chem. Eng. News April 3 (1995) 20.
[24] J.W. Johnson, A.J. Jacobson, J.F. Brody and J.T. Lewandowski, Inorg. Chem 23 (1984) 3842; J.W. Johnson, A.J. Jacobson, W.M. Butler, S.E. Rosenthatl, J.F. Brody and J.T. Lewandowski, J. Am. Chem. Soc. 111 (1989) 381; G. Huan, A.J. Jacobson, J.W. Johnson and E.W. Concoran, Jr., Chem. Mater. 2 (1990) 91; J.W. Johnson, J.F. Brody and R.M. Alexander, Chem. Mater. 2 (1990) 198; G. Huan, J.W. Johnson, A.J. Jacobson and J.S. Merola, Solid State Chem. 89 (1990) 220.
[25] V. Guliants, J.B. Benziger and S. Sundaresan, Chem. Mat. 7 (1995) 1493.